Available online at www.sciencedirect.com
SCIENCE DIRECT®
Thermochimica Acta 417 (2004) 157–161
thermochimica acta
www.elsevier.com/locate/tca

Natural lycopene from *Blakeslea trispora*: all-trans lycopene thermochemical and structural properties

A. Estrella [a], J.F. López-Ortiz [a], W. Cabri [a], C. Rodríguez-Otero [b], N. Fraile [b], A.J. Erbez [c], J.L. Espartero [d], I. Carmona-Cuenca [d], E. Chaves [d], A. Muñoz-Ruiz [d,*]

[a] *Antibioticos, R&D León, Avda. Antibióticos 59-61, 24009 León, Spain*
[b] *Vitatene, Avda. Antibióticos 59-61, 24009 León, Spain*
[c] *Instituto de Ciencia de Materiales de Sevilla, CSIC-USE, C/ Américo Vespucio s/n, Isla de la Cartuja, 41092 Sevilla, Spain*
[d] *Department of Organic Chemistry, Faculty of Pharmacy, C/ Prof. García González, 2, 41012 Sevilla, Spain*

Received 2 October 2003; received in revised form 16 January 2004; accepted 20 January 2004

Available online 5 March 2004

Abstract

Structural and thermal properties of all-trans lycopene are described in the present paper. Different crystalline lycopene samples obtained from fermentation process and recrystallized lycopene were analyzed. Structural properties (NMR, mass spectrometry and powder X-ray diffraction) of lycopene were clarified with recent techniques. High purity sample analysis by differential scanning calorimetry was used to study thermal behavior of pure lycopene and with traces of isomers. But also this was correlated with HPLC method for determine lycopene purity and isomers in low proportion.

Keywords: Lycopene; Carotenoids; NMR; X-ray diffraction; DSC

1. Introduction

Carotenoids are widely spread in nature, being responsible for the characteristic yellow to red colors in many natural products, such as carrots, peppers, tomatoes, flowers and several microorganisms. Lycopene plays an important role in the human diet, and its antioxidants and cancer preventive properties have been proved [1]. Lycopene was typically obtained by chemical synthesis [2] or by extraction from tomato [3]. In most cases of described fermentation using mucoral organisms for the production of lycopene, the product has been a mixture of carotenes including alpha, beta and gamma carotene [4]. However, a fermentation process for obtaining all-trans lycopene as the major product was recently developed in our laboratories. A detailed description of the structural properties and purity analysis is presented in this paper.

2. Materials and methods

Crystalline lycopene samples obtained from the fermentation process were analyzed. Also recrystallization in isobutyl-acetate was done to obtain a high purity lycopene sample (Fig. 1).

2.1. IR

The IR spectrum with KBr plates was obtained on a Perkin-Elmer FT-IR spectrometer SPECTRUM 1000.

2.2. NMR

Samples were examined by NMR spectroscopy as solutions (30 mg/ml) in 99.6% $CDCl_3$. Spectra were recorded at 303 K on a Bruker AMX 500 spectrometer operating at 500.13 MHz (^{1}H) and 125.75 MHz (^{13}C). Chemical shifts are given in parts per million (ppm), using the DMSO-d_6 signals (2.49, and 39.5 ppm for ^{1}H and ^{13}C, respectively) as references. The ^{2}D homonuclear proton double-quantum filtered correlation experiment (DQF-COSY) [5] was performed in the phase-sensitive mode using the Bruker

* Corresponding author. Present address: Department of Pharmaceutics, Faculty of Pharmacy, University of Sevilla, C/ Prof. García González, 2, 41012 Sevilla, Spain. Tel.: +34-95-455-38-05; fax: +34-95-455-67-26.
E-mail address: amunoz@us.es (A. Muñoz-Ruiz).

0040-6031/$ – see front matter © 2004 Elsevier B.V. All rights reserved.
doi:10.1016/j.tca.2004.01.026

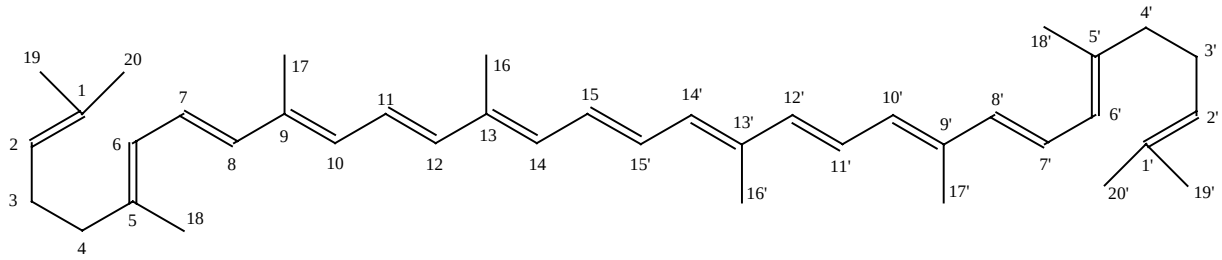

Fig. 1. Lycopene.

standard pulse sequence. The pure absorption ^{2}D NOESY were performed with mixing time of 300 ms. Acquisition and data processing were similar to those used for the DQF-COSY. The ^{2}D heteronuclear one-bond proton–carbon correlation experiment [6] was registered in the ^{1}H detection mode (inverse detection) via single-quantum coherence (HSQC). ^{13}C decoupling was achieved by the GARP scheme. This experiment was slightly modified by the implementation of an editing block in the sequence [7]. The long-range proton–carbon correlation experiment (HMBC) [8] was collected in the ^{1}H detection mode. A delay time of 80 ms between the first and second pulses and 96 scans per increment were used.

2.3. Mass spectroscopy

The CI-MS (thioglycerol + NaI matrix) was obtained on a MicroMass AutoSpeed mass spectrometer.

2.4. Differential scanning calorimetry

A Setaram (Caluire, France) DSC 131 system coupled with a personal computer loaded with the program for processing the results was used. Heat and temperature calibration of the instrument was made by high purity indium and zinc as standard samples. The DSC measurements were carried out with pierced aluminum sample pans and empty reference pans. Both the sample and reference were scanned at a heating rate of 5 K/min from room temperature to 623 K, under nitrogen atmosphere with a flow rate of 25 ml/min. The mass of the sample was 5–10 mg. All measurements were performed at least in duplicate.

2.5. X-ray powder diffraction

Due to the weak dispersing character of the specimen, X-ray diffraction was carried out in transmission mode. The sample was sealed in a Lindemann-glass capillary with 0.5 mm internal diameter. The diffractometer was a Siemens D5000 equipped with a Huber incident beam Germanium monochromator and scintillation counter. The sample was irradiated with Cu Kα1 (0.1541 nm).

2.6. HPLC

The HPLC system is composed of a Waters (Milford, MA, USA) autosampler 717 plus, a Waters 600E multisolvent pump and a Waters 2996 photodiode-array detector. A mobile phase of acetonitrile/methanol (40:60, v/v) with a flow rate of 1.0 ml/min and detection at 470 nm was used to separate lycopene and its *cis* isomers using a Vydac® 218 TP254 (5 μm; 4.6 mm × 250 mm) column. In brief, 25 mg of lycopene standard was dissolved in 10 ml of dichloromethane and then diluted in acetone to get a 0.5% (w/v) concentration. Samples of lycopene crystals were prepared by dissolving the crystals in dichloromethane and diluting with acetone to get a 0.5% (w/v) final concentration.

2.7. Spectrophotometric analysis

A Spectrophotometer Shimadzu UV1603 was used for UV-Vis spectroscopy. Samples of lycopene crystals were prepared by dissolving 15–20 mg of crystals in 10 ml dichloromethane and diluting to 100 ml with *n*-hexane. From this, a 1:100 dilution in *n*-hexane was prepared. Absorbance was measured at 472 nm. The purity was calculated:

$$\%\,\text{lycopene} = \frac{A \times 10,000}{3450 \times P}$$

being A, absorbance at 472 nm, P weight (in g).

3. Results and discussion

3.1. NMR

The chemical shifts in the ^{1}H and ^{13}C NMR spectra of lycopene were assigned from DQF-COSY and HSQC experiments using the Bruker standard pulse sequence (Table 1).

The confirmation of the assignments of ^{1}H and ^{13}C spectra was obtained from ^{1}H to ^{13}C long range correlation NMR experiments (HMBC) (Table 1).

The cross-peaks corresponding to the following long-range couplings have special relevance:

(a) H_{20} with C_{19}, C_2, C_1.
(b) H_{19} with C_{20}, C_2, C_1.

Table 1
^{1}H and ^{13}C NMR data of lycopene[a]

Position	δ_H	δ_C	HMBC[b]
1		131.80	
2	5.11 (t)	123.91	(20), (19), (3)
3	2.11 (s)	26.66	(4)
4	2.11 (s)	40.22	(3)
5		139.52	
6	5.95 (d)	123.13	(18), (4), (7), (8)
7	6.48 (dd)	124.77	(9), (5)
8	6.20–6.28 (m)	135.38	(17), (10), (9)
9		136.15	
10	6.16 (d)	131.52	(17), (8), (12)
11	6.58–6.69 (m)	125.81	(13), (9)
12	6.35 (d)	137.33	(16)
13		136.54	
14	6.20–6.28 (m)	132.63	(16), (15), (13)
15	6.58–6.69 (m)	130.06	(14)
16	1.97 (s)	12.80	(13), (12), (14)
17	1.97 (m)	12.91	(8), (9), (10)
18	1.82 (s)	16.95	(4), (5)
19	1.69 (s)	25.70	(20), (2), (1)
20	1.61 (s)	17.70	(19), (2), (1)

[a] Recorded in $CDCl_3$: chemical shifts are reported as δ values (ppm) from TMS at 500 MHz for ^{1}H and 125 MHz for ^{13}C; signal multiplicity are shown in parentheses.
[b] Carbons showing long-range couplings to proton, $^{n}J_{CH}$ ($n \geq 2$).

(c) H_{17} with C_8, C_9, C_{10}.
(d) H_{16} with C_{13}, C_{12}, C_{14}.

This assignment differs little from that previously reported [9,10], although some differences have been found with Homonuclear Overhauser ^{1}H-NMR.

3.2. X-ray powder diffraction

The following diffractions in Å with their corresponding relative intensities in % were obtained: 7.533 (36.55), 6.083 (42.41), 6.033 (62.41), 5.9400 (52.76), 5.6997 (100.00), 5.4680 (26.90), 5.3000 (90.34), 5.0396 (31.72), 4.7152 (85.17), 4.6573 (41.38), 4.2499 (26.55), 4.1459 (61.72), 4.0594 (55.86), 3.8148 (32.41), 3.6074 (95.52), 3.5425 (39.66), 3.4948 (36.21), 3.1932 (29.31). The crystal structure was earlier described by Mackinney [11]. However, only the following interplanar spaces in Å were reported: 5.79, 5.27, 4.90, 3.97, 3.62 and 3.43. The lack of resolution in former X-ray patterns as well as the presence of other carotenoids and isomers in the samples may cause the differences in the patterns obtained.

3.3. Differential scanning calorimetry

DSC measurements were used both for thermal characterization of lycopene and to determine the relative purity of different lycopene batches. The DSC purity determination is based on the assumption that an impurity will depress the melting point of a pure material whose melting is characterized by a melting point (T_0) and an enthalpy of fusion (ΔH_0). Impurities broaden the melting range and lower the final melting point to a temperature lower than T_0. The effect of an impurity on T_0 is predicted from van't Hoff's law as given in Eq. (1) [12].

$$T_m = T_0 - \frac{RT_0^2\chi_2}{\Delta H_0}\frac{1}{F} \quad (1)$$

where T_m is the sample temperature at equilibrium, T_0 the melting point of the pure component, R the gas constant, χ_2 the mole fraction of impurity and F is the fraction molten at T_m.

Ford and Timmins [13] described the effect of purity on peak shape and according to van't Hoff's law developed Eq. (2) for curve analysis. A plot of sample temperature (T_s) versus reciprocal F (using only the portion up to the vertex of the peak, as Barral and Diller recommend [14]) should give a straight line of slope equal to the negative of the melting point depression ($T_0 - T_m$). The melting point depression is proportional to the difference in purity in different batches:

$$T_s = T_0 - \frac{T_0 - T_m}{F} \quad (2)$$

The DSC curve (Fig. 2) of the purest batch of lycopene (99% purity), shows no other significant artifacts but an

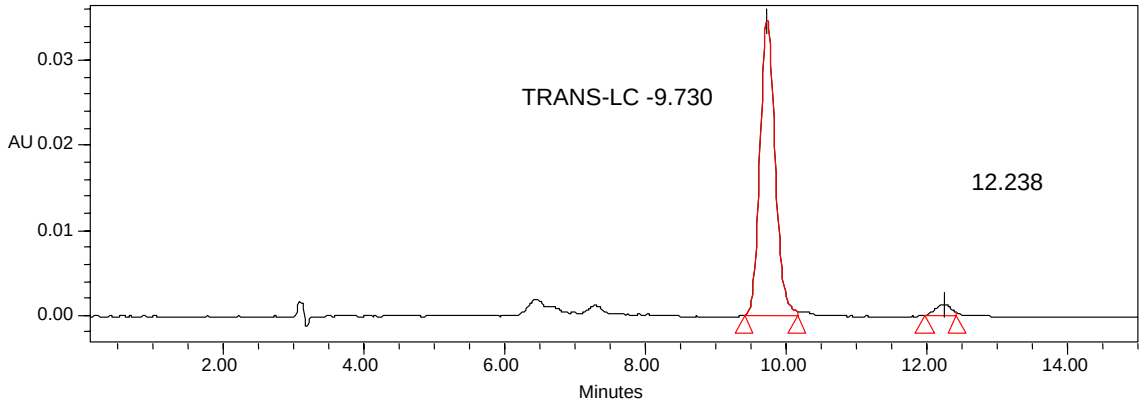

Fig. 2. Typical HPLC profile of lycopene from *Blakeslea trispora*.

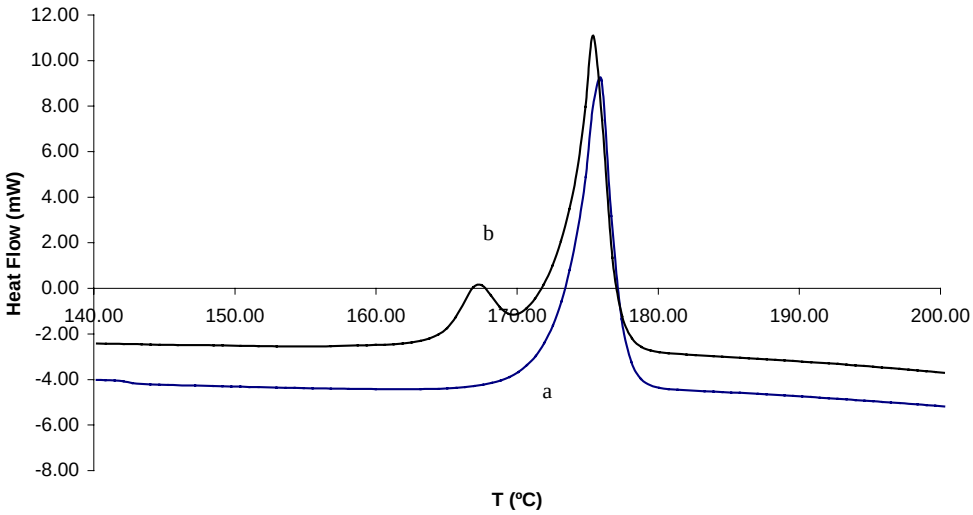

Fig. 3. DSC curve of lycopene 99% pure (a) and a lycopene batch with 5.9% of impurity (b).

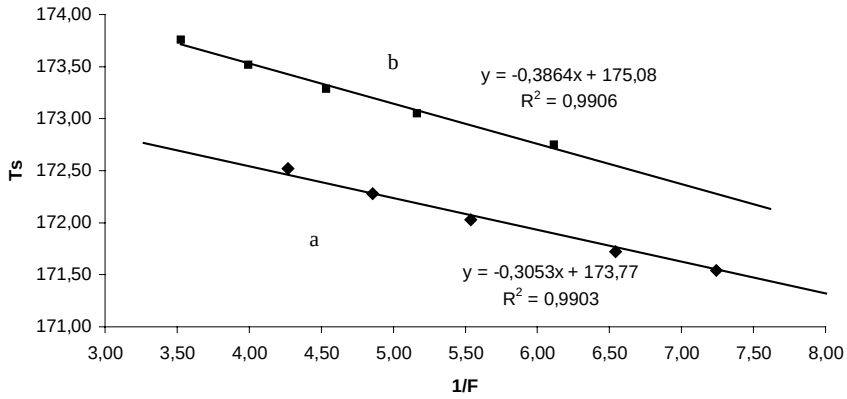

Fig. 4. T_s vs. $1/F$ in two batches with 3.56% impurity (a) and 5.80% impurity (b). The slope of each straight line gives the temperature depression due to the presence of the impurity in the sample.

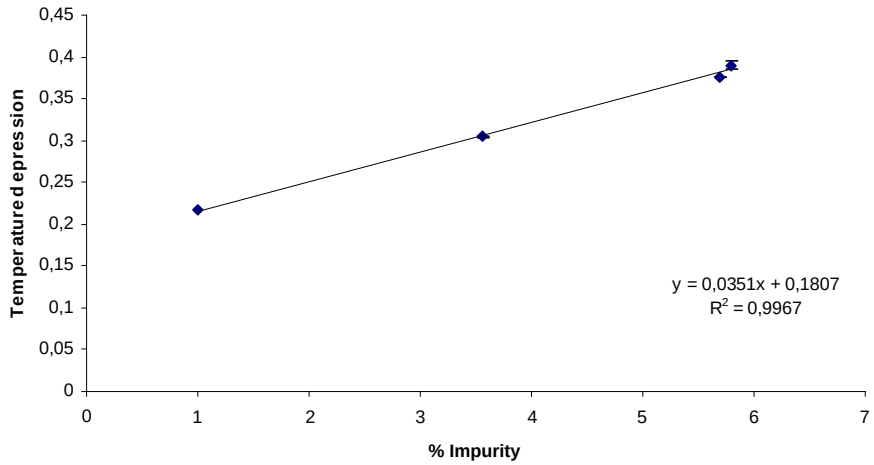

Fig. 5. Temperature depression on the melting point vs. level of impurity the lycopene batches.

endothermic melting curve described by an onset point of 173.23 °C, peak at 175.80 °C and a total enthalpy of fusion of 85.17 J/g (area under the peak). Pure substances have their melting point at the onset temperature of the melting curve. Thus, the melting point of lycopene according to DSC measurements is 173.23 °C. This value was between 171 and 176 °C previously reported by Sumartis and Ofner [15] and Manchand et al. [16]. The presence of eutectic impurities broadens the main melting peak and lowers the vertex temperature. Furthermore, the impurity yields another smaller peak whose area correlates with the proportion of such impurity in the sample (Fig. 3).

Plotting T_s versus reciprocal F of all batches, the slope of each plot gives the melting point depression of each batch. An example of such plot is shown in Fig. 4 where two batches with impurities of 3.56% (a) and 5.80% (b) are compared.

A plot of percentage of impurity (obtained by HPLC method described below) versus melting point depression was drawn, obtaining a linear relation as theoretically expected (Fig. 5). Four batches with different degree of purity were evaluated, yielding a linear relation between the temperature depression and the percentage of impurity, as Eq. (2) predicts (see Fig. 5). Thus, the proportion of impurity is proportional to the melting point depression. This shows a linear relation between both HPLC and DSC techniques. Furthermore this correlation confirms the precision of the HPLC analytical method and the improvement with other analytical HPLC of isomers applied in Food Science [17].

Acknowledgements

Authors thank to Ministerio de Ciencia y Tecnología (Spain) for support under auspices of Material Research program (MAT 2002-02834) and Ministerio de Industria for support under PROFIT projects.

References

[1] S.K. Clinton, Nutr. Rev. 56 (1998) 35–51.
[2] J.E. Johansen, S. Liaaen-Jensen, Acta Chem. Scand. B28 (1974) 301–307.
[3] D.J. Hart, K.J. Scott, Food Chem. 54 (1995) 101–111.
[4] M.E. Rafelson, J. Bacteriol. 95 (1968) 426–432.
[5] D.J. States, R.A. Haber Korn, D. J Ruben, J. Magn. Reson. 48 (1982) 286–292.
[6] G. Bodenhausen, D. Ruben, J. Chem. Phys. Lett. 69 (1980) 185–189.
[7] T. Parella, F. Sánchez-Ferrando, A. Virgili, J. Magn. Reson. 126 (1997) 274–277.
[8] M.H. Frey, W. Leupin, O.W. Sorensen, W.A. Denny, R.R. Ernst, K. Wüthrich, Biopolymers 24 (1985) 2371–2380.
[9] G. Englert, Helv. Chim. Acta 62 (1979) 1497–1500.
[10] U. Hengartner, K. Bernhard, K. Meyer, Helv. Chim. Acta 75 (1992) 1848–1865.
[11] G. Mackinney, J. Am. Chem. Soc. 56 (1934) 488.
[12] USP 23, NF 18, Therm. Anal. (1995) 1837–1838.
[13] J.L. Ford, P. Timmins, Pharmaceutical Thermal Analysis: Techniques and Applications, Ellis Horwood Limited, 1989, pp. 108–135.
[14] E.M. Barral II, R.D. Diller, Thermochim. Acta 1 (6) (1970) 509–520.
[15] J.D. Sumartis, A.J. Ofner, J. Org. Chem. 28 (1963) 2735–2739.
[16] P.S. Manchand, R. Rüegg, U. Schwieter, P.T. Sidons, B.C.L. Weedon, J. Chem. Soc. (1965) 2019–2026.
[17] T. Anguelova, J. Warthensen, J. Food Sci. 65 (2000) 67–70.